CHAPTER 5

The Future and Recovery

Convening Lead Author: Malcolm Ko, NASA

Lead Authors: John S. Daniel, NOAA; Jay R. Herman, NASA; Paul A. Newman, NASA; V. Ramaswamy, NOAA

KEY ISSUES

This chapter presents results on how future halogen loading is expected to affect the behavior of total column ozone and the prospect for the detection/validation of the anticipated recovery trend. In a hypothetical argument, if circulation, climate, and the background atmosphere were to remain unchanged as of the present-day, the projection of ozone could be based essentially upon future halogen loading. However, the reality is that the concentrations of other trace gases that affect ozone (*e.g.*, methane [CH_4], nitrous oxide [N_2O], and water vapor) are changing because of changes in emissions; climate, which also affects ozone abundances, is changing as well. The model-simulated results show that the ozone increase expected between now and 2025 is largely due to the anticipated decrease in halogen loading, and ozone-depleting substances (ODSs) will remain one of the drivers of human-caused ozone depletion up until the middle of the twenty-first century, when the halogen loading is expected to approach its 1980 value. Reductions in emissions of these chemicals represent the only known currently acceptable method to reduce this depletion in this period. The effects of climate change (largely driven by increases in carbon dioxide, CO_2) and changes in other trace gases (*e.g.*, CH_4, N_2O, and hydrofluorocarbons) will play an increasing role in the ozone behavior.

Ozone is only one of many factors that affect UV (ultraviolet radiation) at the surface. Future changes in UV will be discussed in this chapter in the context of the projected ozone change in the stratosphere. The Equivalent Effective Stratospheric Chlorine (EESC) is used to compare the relative impacts of various ODS emissions scenarios on future ozone. Included in this discussion is the radiative forcing associated with the halocarbons as well as the hydrofluorocarbons (HFCs) used as replacements for the ODSs. The contribution from the United States to the future halocarbon loading will be addressed in the context of EESC and radiative forcing.

The key issues, in the form of questions, that are addressed in this chapter include:

- What is the future behavior of ozone as predicted by numerical models?
- What is the future behavior of ultraviolet radiation at the Earth's surface?
- Are there any new findings concerning projected future emissions of ODSs?
- What is the radiative forcing associated with ODSs and HFCs emitted as replacement chemicals for the ODSs and how will it likely change in the future?
- To the extent that the emissions from a specific country can be used to estimate its contribution to global ozone depletion and radiative forcing by ODSs and their replacements, what is the United States' contribution?

Key Findings

Equivalent Effective Stratospheric Chlorine (EESC) is a useful index for comparing relative merits of different halocarbon emission scenarios in minimizing ozone depletion. Current scenarios being considered include projected emissions of long-lived source gases only and do not include emissions of very short-lived source gases.

- The time for EESC to return to the 1980 level (the EESC recovery date) and the integrated EESC values (to the EESC recovery date) provide useful metrics to compare the relative merits of various emissions scenarios.
- There have been suggestions that the mean age of air, and age-dependent release factors should be used in the calculation of EESC. This is potentially useful for calculating EESC values that are more representative of polar ozone depletion, in particular. The new recipe will change the absolute values of the metric for global ozone depletion, but should not qualitatively affect the relative benefit estimates of the different scenarios.

Two-dimensional chemistry transport models (both with and without climate feedback) and three-dimensional climate chemistry models (3-D CCMs) were used to simulate the behavior of ozone in the twenty-first century using the WMO (2003) baseline scenario.

The scenario includes changes arising from natural and anthropogenic activities other than ODS emissions. Thus, it is expected that the model-simulated ozone recovery date will differ from the EESC recovery date. The model-simulated ozone results will be discussed in the context of the EESC recovery date between 2040 and 2050 for midlatitudes, and between 2060 and 2070 for the polar regions. Analyses of simulation results indicate that:

For the model-simulated ozone content between 60°N and 60°S :

- Between now and 2020, the simulated total ozone content will increase in response to the decrease in halogen loading.
- Some 3-D CCMs predict that stratospheric cooling and changes in circulations associated with greenhouse gas emissions will enable global ozone to return to its 1980 value up to 15 years earlier than the EESC recovery date.
- Based on the assumed scenario for the greenhouse gases (which includes CH_4 and N_2O), the ozone content between 60°N and 60°S is expected to be 2% above the 1980 values by 2100. Values at midlatitudes could be as much as 5% higher.

For the model-simulated Antarctic ozone:

- The model-simulated ozone recovery date (the year when ozone returns to its 1980 value) for Antarctic ozone behavior depends on the diagnostics chosen. The minimum ozone value is projected not to start increasing until after 2010 in several models, while a decrease in ozone mass deficit in most models has occurred by 2005.
- Model simulations show that the ozone amount in the Antarctic will reach the 1980 values 10 to 20 years earlier than the 2060 to 2070 time frame.

For the model-simulated Arctic ozone:

- Ozone in the Arctic region is expected to increase. Because of large interannual variability, the simulated results do not show a smooth monotonic recovery. The dates of the minimum column ozone from different models occur between 1997 and 2015.
- Most CCMs show ozone values at 2050 larger than the 1980 values, with the recovery date between 2020 and 2040.
- Results from the majority of the models indicate that Arctic ozone depletion will not be significantly worse than what has already occurred.

With the current scenarios, anthropogenic halogens identified in the Montreal Protocol should have a minimal effect on midlatitude ozone beyond 2050. In order to predict the future trend of ozone in that time frame, one must consider projections for climate changes and changes in trace gases such as other halogens, CH_4, and N_2O.

Applying ozone trend analysis techniques to future observations should enable one to confirm the time when halogen loading has minimal influence on global ozone within five to ten years after it occurs.

The future UV trend at the surface is likely to be more dominated by changes in clouds, aerosols, and tropospheric air quality than by ozone changes in the stratosphere. Equivalent Effective Stratospheric Chlorine (EESC) will still be a useful predictor for the relative effects of ODSs on future UV in terms of evaluating the different scenarios.

Future halocarbon emissions are derived using a new bottom-up approach for estimating bank sizes. The new method gives future chlorofluorocarbon (CFC) emissions that are higher than previously estimated in WMO (2003).

- Current projected concentrations for EESC in the twenty-first century are higher than reported in WMO (2003) because the most recent CFC bank estimates, which are believed to be more accurate, are larger and lead to larger emissions, and the estimated emissions due to future production of hydrochlorofluorocarbons (HCFCs) from Article 5(1) countries are also larger.
- The EESC in the baseline scenario returns to the 1980 value in the year 2049, about five years later than the date based on the WMO (2003) baseline scenario.
- Compared to the WMO (2007) baseline scenario, cessation of all future emissions will bring the EESC recovery date earlier by 15 years to 2034. Integrated EESC (from 2007 to the EESC recovery date) from ODSs already in the atmosphere as of 2007 is 58% of the integrated EESC for the baseline scenario.
- If no future ODS production is assumed, the date when EESC returns to the 1980 level is moved earlier by six years to 2043. The integrated EESC from ODSs produced after 2007 is 17% of the integrated EESC for the baseline case.

Direct radiative forcing from ODSs and HFC replacement chemicals is approximately 0.34 W per m^2 in 2005 and is expected to stay below 0.4 W per m^2 through 2100 (according to the WMO (2007) scenario for ODSs and the IPCC Special Report on Emission Scenarios (SRES) scenarios considered for HFCs). This is to be compared with forcing from CO_2 of 1.66 W per m^2 in the 2005 atmosphere, increasing to as high as 5 W per m^2 by 2100 for the SRES A1B scenario.

- Direct forcing from CFCs will decrease to 0.1 W per m^2 by 2100. Direct forcing from HCFCs and other anthropogenic ODSs is expected to be negligible by 2100.
- Forcing from HFCs is 0.15 W per m^2 and 0.24 W per m^2 in 2050 and 2100, respectively, for the SRES A1B scenario, whereas other scenarios indicate that it will be lower. However, current observations suggest that the present atmospheric radiative forcing of the HFCs has been larger than computed for the SRES scenarios, primarily due to higher HFC-23 concentrations.

The forcing associated with the observed ozone depletion was estimated to be about –0.05±0.10 W per m^2 in 2005, corresponding to one-sixth of the direct forcing due to ODSs.

If one assumes that all of the observed ozone depletion is due to ODSs, that would imply that the indirect effect of ODSs due to ozone depletion is one-sixth of the direct effects for the mix of ODSs present in the atmosphere at that time. Current estimates assume that the indirect forcing from ODSs will decrease to zero approximately when EESC returns to its 1980 levels, while the direct forcing (mainly from CFCs and HFCs remaining in the atmosphere) will continue. The indirect forcing remains highly uncertain and is discussed in more detail in Chapter 2.

Using available historical and projected United States and global emissions estimates, we find that emissions from the United States contribute between about 15% and 37% to global EESC due to man-made emissions at 2030. For the same year, the United States' contribution to direct radiative forcing from ODSs, HFCs, and PFCs (perfluorocarbons) is 19% to 41%.

5.1 INTRODUCTION

This chapter presents results on how future halogen loading will affect the future behavior of total column ozone and the prospect for the detection/validation of the expected recovery trend. In a hypothetical argument, if the transport circulation, the climate, and the background atmosphere were to remain unchanged as of the present-day, the projection of ozone could be based essentially upon future halogen loading. Chapter 2 discussed the concept of Equivalent Effective Stratospheric Chlorine (EESC) and how the values for midlatitude EESC and polar EESC could be used as metrics to approximate the effects of ODSs on ozone behavior. Daniel *et al.* (1995) pointed out that global stratospheric ozone losses became apparent from observations around the late 1970s to around 1980 (see also Figure 3.2 in this report). They also considered that the total ozone over Halley Bay dropped nearly linearly from 1980 to 1990. From these facts, they assumed that the ozone trend due to halogen loading was close to zero for EESC smaller than the 1980 value. If one assumes that the same holds for the future and nothing else is different, ozone is expected to recover to the 1980 value at the same time as EESC. The time for EESC to return to its 1980 value thus has been adopted as a metric to compare various control options. For this reason, the date when the future EESC value returns to its 1980 value is given some significance, and is referred to as the EESC recovery date (EESC RD).

The decreasing trend in ozone during the period 1964 to 2006 can be mostly attributed to the increase in halogen loading. It is anticipated that the decrease in halogen loading in the next 20 years will have a large influence on the decadal trend of ozone.

Since policy decisions are being made based on EESC, it would be prudent to perform analyses to see how well the EESC-based predictions correlate with model simulations of ozone recovery. Unfortunately, the scenarios used in the model simulations reported in WMO (2007) include changes in trace gases other than the halogens that affect ozone directly through chemical interactions, or indirectly through climate change. Thus, the model-simulated ozone recovery date (MS ORD, *i.e.*, the date ozone returns to its 1980 value) for these simulations is expected to be different from the EESC RD.

The results of numerical simulations of the future behavior of ozone as reported in the WMO (2007, Chapter 6) report are presented in Section 5.2. A discussion of how future observed ozone behavior can be used to detect and confirm the ozone recovery date is presented in Section 5.2.3. Section 5.3 discusses how future ozone may affect UV. Sections 5.4 and 5.5 focus on expected future trends of the halocarbons through 2050. The future emissions and abundances of the CFCs and HCFCs are discussed in Section 5.4. The EESC will be used to compare the relative impacts of various ODS emissions scenarios on future ozone in Section 5.5. Included in this section is a discussion of the radiative forcing associated with the ODSs as well as the HFCs used as replacements for them. The contribution from the United States to the global future halocarbon loading will be addressed in the context of EESC and radiative forcing in Section 5.6.

5.2 MODEL SIMULATIONS AND ANALYSES OF OZONE BEHAVIOR

Analyses of the over 40-year time series of global ozone data between 1964 and 2006 (see discussion in Chapter 3, Figure 3.2) indicate that it is possible to attribute the observed ozone behavior to several processes that affect ozone. These include the responses to the seasonal cycle, to the quasi-biennial oscillation (QBO), to the 11-year solar cycle, to episodic volcanic eruptions, and to halogen loading from halocarbons. In particular, most of the decreasing trend in ozone during this period can be correlated with EESC and attributed to the increase in halogen loading. It is anticipated that the decrease in halogen loading in the next 20 years will have a large influence on the decadal trend of ozone. To predict the future trend of ozone, one must identify all processes that may affect ozone, determine how the driving mechanisms may change (*i.e.*, the scenarios), and employ numerical models to simulate the ozone behavior. The projected behavior will depend on the adopted scenario. The results presented in this section also show that different models predict different results for the same scenario. This indicates that there is still disagreement on how processes are represented in the models, and one must depend on further comparison with observations to resolve these issues. Finally, the purpose for presenting the model results in this chapter is to illustrate, in general terms,

how the expected ozone behavior differs from the parameterized behavior based on EESC. It is beyond the scope of this report to address the various outstanding issues associated with simulating ozone behavior. Such attempts would greatly benefit from studies of changes in local ozone as functions of altitude.

5.2.1 Processes and Scenarios Used in Model Simulations

It is clear that the model simulations must include the effects from changes in halogen loadings. The model simulations use prescribed surface concentrations of the halocarbons derived from projected emissions. The method for deriving the surface concentrations from emissions will be discussed in more detail in Section 5.4. The current best-estimate scenario for future halocarbon emissions (A1) is discussed in Table 8-4 and the surface concentrations are summarized in Table 8-5 of the WMO (2007, Chapter 8) report. Note that this scenario, as with all other scenarios previously considered in the WMO reports, considers only relatively long-lived (lifetime > 0.5 years) chlorine and bromine source gases. However, it has become clearer that very short-lived (VSL) ODSs also contribute to stratospheric ozone depletion, particularly short-lived bromocarbons. A more detailed discussion of the contribution of VSL compounds to stratospheric chorine and bromine loading can be found in Chapter 2 of WMO (2007). Note that the standard procedure for estimating EESC from emissions of long-lived source gases (Box 2.7 in Chapter 2 of this report) should not be applied to VSL source gases in its current form. It was estimated in WMO (2007) that VSL compounds might contribute 50 ppt (parts per trillion by mole) of stratospheric chlorine and 3 to 8 ppt of stratospheric bromine. It was unclear whether any trend in these VSL compounds should be expected in the future or has occurred in the recent past. Enhancement in convective activities associated with future climate changes may increase the Ozone Depletion Potentials (ODPs) of the VSL species.

Because the chapters in the WMO (2007) report were prepared in parallel, there was not sufficient time to use this most updated scenario in the model simulations. The model results presented in Chapter 6 of the WMO (2007) report were simulated using the scenario (Ab) as summarized in Table 4B-2 in the WMO (2003, Chapter 4) report. Using assumed values for the atmospheric lifetimes, the release factors of the halocarbons, and the transport lag from the tropopause, one can compute the date when midlatitude and polar EESC will reach its 1980 value. For scenario Ab, the midlatitude EESC RD is calculated to be 2044. However, because of the uncertainties associated with the lifetimes and the release factors, Chapter 6 of the WMO report chose to discuss the results relative to an EESC RD range between 2040 and 2050. The model-simulated ozone recovery date (MS ORD) could be earlier than the EESC RD if the net effect from other non-ODS factors (see below) causes an increase in ozone relative to the 1980 value. Finally, the MS ORD for ozone at specific latitudes is likely to be different for different latitudes.

Note that even in simulations that keep all other parameters the same except for halogen loading, the EESC RD and MS ORD is still likely to be different because the lifetimes, the release factors, and the bromine efficiency factor in the model are likely to be different from what are assumed in the EESC calculation. To resolve this issue, comparison and validation of model-simulated atmospheric lifetimes and release factors should be a priority. Until this is accomplished, direct comparison between the EESC RD with the MS ORD is not as meaningful as it could be.

Variations in natural factors such as changes in the Sun's energy output and volcanic events will continue to have impacts on the ozone abundances.

Variations in natural factors such as changes in the Sun's energy output and volcanic events will continue to have impacts on the ozone abundances. Changes in solar UV between solar cycles are assumed to be small. Effects on ozone from variations within each 11-year cycle can be isolated as demonstrated in Figure 3.2. Once identified, the effect can be removed in interpreting the observed ozone changes. Thus, it is not crucial whether the solar cycle effect is included in the simulations. Effects from volcanoes are not included as there is no reliable way to predict volcanic eruptions in the future. Their effects can be removed in the analyses several years after it occurs. The philosophy here is that, like the solar cycle, the effect can be removed from the observation before they are compared with the model simulated trends.

Chapter 4 discussed how climate change due to increased CO_2 (and other well-mixed greenhouse gases), changes in water vapor in the stratosphere, and changes in long-lived source gases (CH_4 and N_2O) could affect ozone. Climate change can affect ozone through changes in temperature and transport circulation. Cooling of the stratosphere associated with greenhouse gases is expected to slow gas-phase ozone loss reactions and increase ozone. This is particularly effective in the upper stratosphere. Water vapor in the stratosphere plays a particularly interesting role. It affects ozone concentration through the odd-hydrogen (HO_x) chemistry, as well as contributing to the cooling of the stratosphere. Its concentration can be changed due to changes in methane and changes in climate. In the scenario calculations, changes in water are not prescribed. They are calculated from the CH_4 increase and from changes associated with climate in chemistry climate models (CCMs).

Climate change can affect ozone through changes in temperature and transport circulation. Cooling of the stratosphere associated with greenhouse gases is expected to slow gas-phase ozone loss reactions and increase ozone.

The scenario for CO_2, CH_4, and N_2O used in the simulations is summarized in Table 5.1. Based on sensitivity simulations from two-dimensional (2-D) chemistry transport models (CTMs) reported in WMO (1999, Chapter 12), a 15% increase in CH_4 at 2050 from its 2000 values would have added about 0.5% in column ozone at midlatitudes. A 15% N_2O increase would have decreased ozone by about 1%. Thus, in the scenario shown, the combined effects from CH_4 and N_2O increase ozone around 2050.

The WMO reports also discussed changes in aerosol and oxides of nitrogen (NO_x) from aviation (WMO, 2003, Chapter 4), emissions from rocket launches (WMO, 2003, Chapter 4), and changes in molecular hydrogen (H_2) (WMO, 2007, Chapter 6). The effects from these processes are not included in the WMO simulations. Emission of NO_x from subsonic airplanes increases ozone in the upper troposphere. The IPCC (1999) estimates that a 0.4% increase in column ozone at midlatitudes in the current atmosphere can be attributed to en route emissions from aircraft. Anticipated doubling to tripling of emissions by 2050 could add another 1%. Detailed projections of future emissions based on demands and technology advances are not yet available. Previous estimates suggest that the current rocket launch schedule may have caused a small (less than 1%) column decrease due to loss in the lower stratosphere. Future trends will depend on growth and mix of solid fuel and liquid fuel propellants. Estimates for changes in H_2 are based on the assumption that liquid hydrogen may become an important energy source for the economy and leakage from storage and usage may cause a dramatic increase in H_2. Not enough is known to do any reliable projections.

5.2.2 Results From Model Simulations

Three types of models were used to simulate the future behavior of ozone in WMO (2007, Chapter 6):

1. Two-dimensional chemistry-transport models (2-D CTMs) use fixed temperature and circulation. They are most useful for isolating the effects of different source gases;
2. Interactive 2-D models partially account for the changes in transport associated with climate change by calculating the residual circulation from heating rates allowing for interaction of planetary waves with the mean circulation. However, the feedback from changes in wave forcing is not simulated; and
3. Three-dimensional climate chemistry models (3-D CCMs) incorporate all the identified feedbacks and are generally

Table 5.1 Future concentrations of CO_2, CH_4, and N_2O used in the model simulations. The CO_2 values are from the Integrated Science Assessment Model (ISAM) as listed in Appendix II of IPCC (2001).

Year	2000	2010	2020	2030	2040	2050	2060	2070	2080	2090	2100
CO_2 (ppm)	369	391	420	454	491	532	572	611	649	685	717
CH_4 (ppb)	1760	1871	2026	2202	2337	2400	2386	2301	2191	2078	1974
N_2O (ppb)	316	324	331	338	344	350	356	360	365	368	372

better able to represent the key processes related to 3-D transport in the atmosphere (particularly the polar regions).

In the following discussion, both the observations and the model results will be displayed as annual mean or monthly anomalies expressed as a percentage of the pre-1980 conditions. The midlatitude EESC RD is expected to occur sometime between 2040 and 2050. In looking at the MS ORD, it has proven convenient to examine the spatial aspects of the problem in terms of the phenomena in the two polar regions (Arctic and Antarctic) and that in the tropics plus midlatitudes (approximately 60°N to 60°S). This separation accounts for the distinct stratospheric circulation patterns prevailing in the climate system, is relevant for compartmentalizing approximately the ozone chemical-dynamical interactions, and represents a convenient way to look at the "big" global picture.

5.2.2.1 Tropics and Midlatitudes

Figure 5.1 shows the simulated future behavior of column ozone from interactive 2-D models (solid lines) and non-interactive 2-D CTMs (dashed lines). The models' hind-cast predictions are compared with observations as a way to screen the 2-D CTMs. All 2-D models show that ozone amount increases with time between 2007 and 2050. The model spread among the non-interactive 2-D CTMs for northern midlatitudes is about 3% at 2050. The WMO (2007, Chapter 6) report did not discuss how changes in N_2O and CH_4 contributed to the individual model results. Based on the estimates given above and the scenario stated in Table 5.1, it would appear that CH_4 is adding about 1% while the effect of N_2O is to decrease ozone by about 0.5% in 2050. It is also evident from the figure that the sensitivities in these models differ.

Results from the interactive 2-D models show that the ozone anomaly is larger by about 2% in 2050 and 4% in 2100. The effect at midlatitudes is larger at about 3% in 2050. This is consistent with the expected ozone increase due to cooling in the stratosphere. There is no clear indication on the effect of increased upwelling in the tropics, though this could have been masked by the ozone increase in the upper stratosphere due to the cooling.

Results from 3-D CCMs are shown in Figure 5.2. Several tests were used to identify models that successfully simulate parameters important for ozone response to halogen loading (Eyring *et al.*, 2006). Models that perform better in those tests are identified using solid lines in Figure 5.2. For our purpose, we concentrate on the three models (CCSRNIES, CMAM, and WACCM) that "earned" the solid line rating and performed the REF2 simulations from 1980 to 2050. Other models performed the REF2 simulation starting in 1990 or 2000 making it difficult to compare the ozone anomaly at 2050 to the anomaly at 1980 to determine the

All two-dimensional models used to simulate the future behavior of ozone show that ozone amount increases with time between 2007 and 2050.

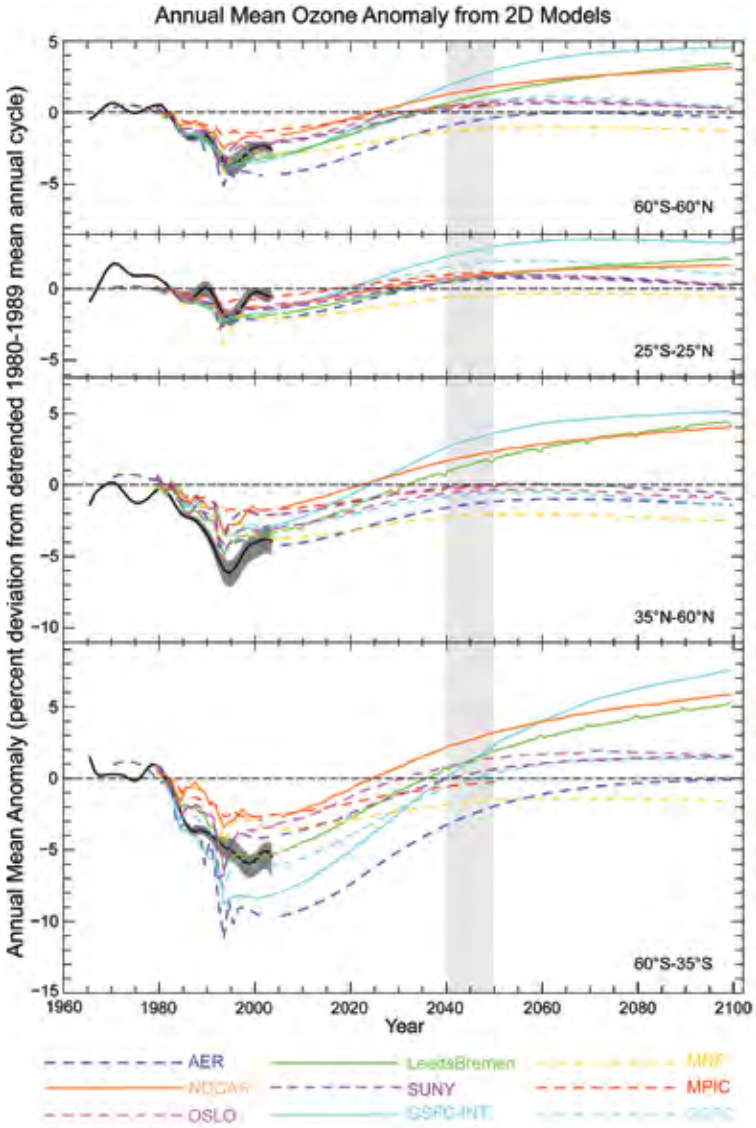

Figure 5.1 Simulated annual mean ozone anomaly from 2-D models for different latitude bands. Results from interactive models are designated by solid lines. The figure is based on Figure 6-9 in WMO (2007). See Eyring *et al.* (2006) for details on how the annual mean anomaly is computed. The black line with the grey shade represents the observed mean values and the range. The grey vertical band marks the time period when midlatitude EESC is expected to recover to the 1980 value.

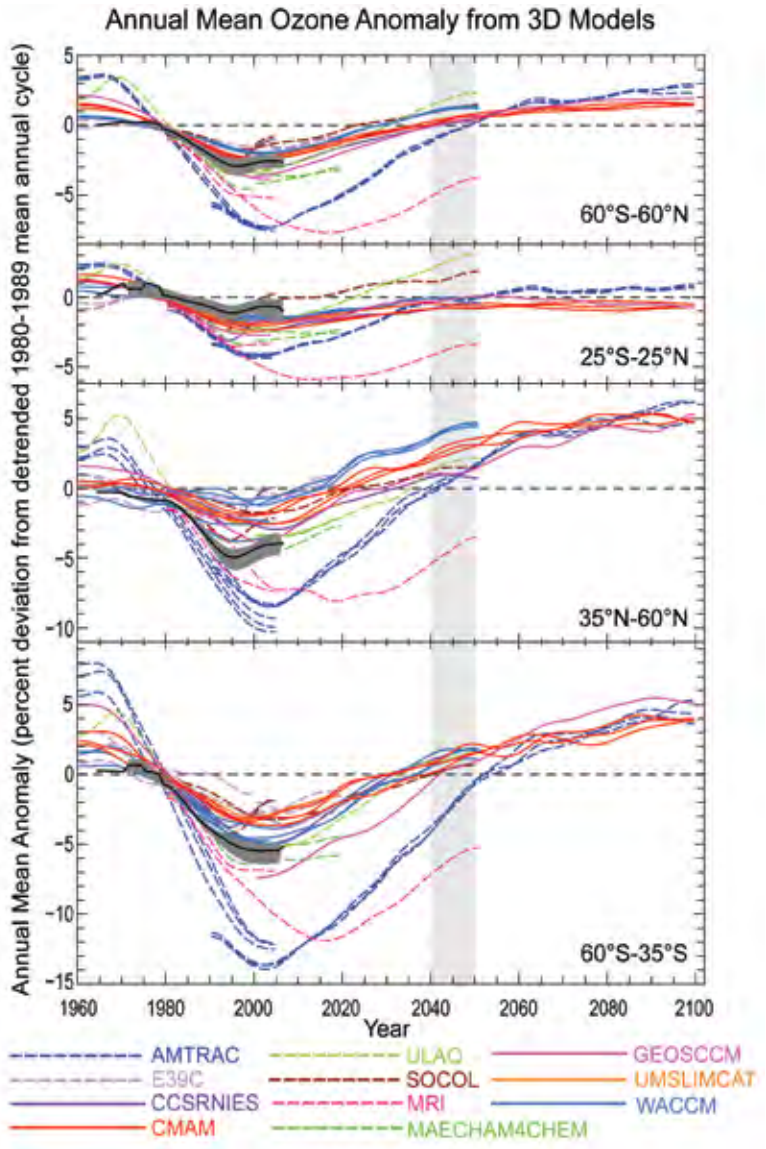

Figure 5.2 Results from 3-D CCMs. The figure is adapted from Figure 5 in Eyring *et al.* (2007) which includes additional model results computed after publication of the WMO (2007) report. See Eyring *et al.* (2006) for details on how the annual mean anomaly is computed. The solid line with the grey shade represents the observations with uncertainty. The grey vertical band marks the time period when midlatitude EESC is expected to recover to the 1980 value.

Almost all 3-D models predict that the Arctic ozone recovery date is much earlier than the Antarctic recovery date.

MS ODR. For ozone content between 60°S and 60°N, the MS ORD are 2030 for WACCM and 2040 for CMAM and CCSRNIES. All three models show little ozone increase beyond the 1980 values in the tropics, consistent with the expectation that increase in upwelling is suppressing ozone. This is evident in the model-simulated decrease in tropical ozone below 20 hectopascals (hPa) (see Figure 6[b] in Eyring *et al.*, 2007). The MS ORDs for northern midlatitudes are 2010 for WACCM, 2020 for CMAM, and 2030 for CCSRNIES. The MS ORDs for the southern midlatitudes are all between 2030 and 2040. The CMAM model presented results through 2100.

To isolate the effects of climate change, three CCMs performed a simulation where the surface concentrations of the greenhouse gases (GHGs) were kept fixed at their 1970 value (Figure 5-25 in Chapter 5, WMO, 2007). The results from WACCM show that in the absence of these GHG forcings, the MS ORD for 60°S to 60°N is around 2040 and the ozone amount in 2050 is about 1% smaller compared to the baseline scenario that includes the GHG forcings. Unfortunately, the run also kept the surface concentrations of CH_4 and N_2O fixed. Thus, the 1% effect results from both climate change and the direct chemical effects of CH_4 and N_2O.

5.2.2.2 Polar Region

Figure 5.3 shows the model-simulated ozone anomalies for the Arctic and the Antarctic regions. Most models show larger anomalies in the Antarctic, consistent with the fact that the temperature is colder, leading to formation of more polar stratospheric clouds (PSCs), and the vortex is more confining. Within almost all models, the Arctic ozone recovery date is much earlier than the Antarctic ozone recovery date.

The polar EESC RD is estimated to be between 2060 and 2070. We will again concentrate on the results from CCSRNIES, CMAM, and WACCM for the reason discussed in the previous section. The MS Arctic polar ORDs are 2000 for CCSRNIES, 2010 for CMAM, and 2015 for WACCM. Once the ozone anomaly reaches the 1980 value, it increases smoothly to beyond the 1960 anomaly.

The exact time evolution of the Antarctic ozone hole is different depending on the diagnostics chosen. These include ozone amount in October, minimum ozone in September and October, ozone mass deficit, and maximum Antarctic ozone hole area between September and October. The minimum ozone value is projected not to increase until after 2010 in several models, while the decrease in ozone mass deficit in most models has occurred by 2005. If we use the ozone content poleward of 60° calculated by the three models as the metric, the MS ORDs are up to 30 years earlier. The CMAM and WACCM

models produced ensemble results. The three simulations from the WACCM model produced polar ozone recovery dates between 2030 and 2040, while those from CMAM are between 2040 and 2060. The CMAM results also showed that the value for the Antarctic ozone anomaly stays closed to zero for about 20 years after the initial recovery before taking off.

5.2.3 Stages of Ozone Recovery From ODSs

The model-simulated results presented in Figure 5-25 in Chapter 5 of WMO (2007) suggest that the ozone increase between now and 2025 is largely due to the decrease in halogen loading. ODSs will remain a driver of human-caused ozone depletion up until 2040, and reductions in emissions of these chemicals represent the only known acceptable method to reduce the associated ozone depletion expected in this period. The halogen loading is expected to approach its 1980 value toward the middle of the century at midlatitudes. In the decades that follow, the effects of climate change and changes in other trace gases will determine the ozone behavior.

A good portion of Chapter 6 in the WMO (2007) report was devoted to discussion of the detection and attribution of the expected ozone recovery based on future observations. Because of interannual variability, it is not possible to identify an ozone recovery date from observation as soon as it occurs. If one were able to isolate the trend due to halogen loading from the observed ozone time series, one would expect this trend to first stop decreasing when EESC peaks (around 1997 for midlatitudes), followed by an increasing trend until the trend becomes zero again when halogen loading no longer has an effect on ozone. This is the trend-derived halogen-induced ozone recovery date (TD H-ORD). The work of Weatherhead *et al.* (2000) and Yang *et al.* (2006) clearly show that the length of observations required to detect such change depends on the quality of the data. Given the current results, it is anticipated that we should be able to confirm whether ozone is increasing due to decrease in halogen loading in the next five or six years. We are not in a position to recognize the TD H-ORD as soon as it occurs. Nonetheless, the simulations give confidence that one should be able to confirm the ozone recovery after the fact by waiting several years to analyze the observations and removing the interannual variability.

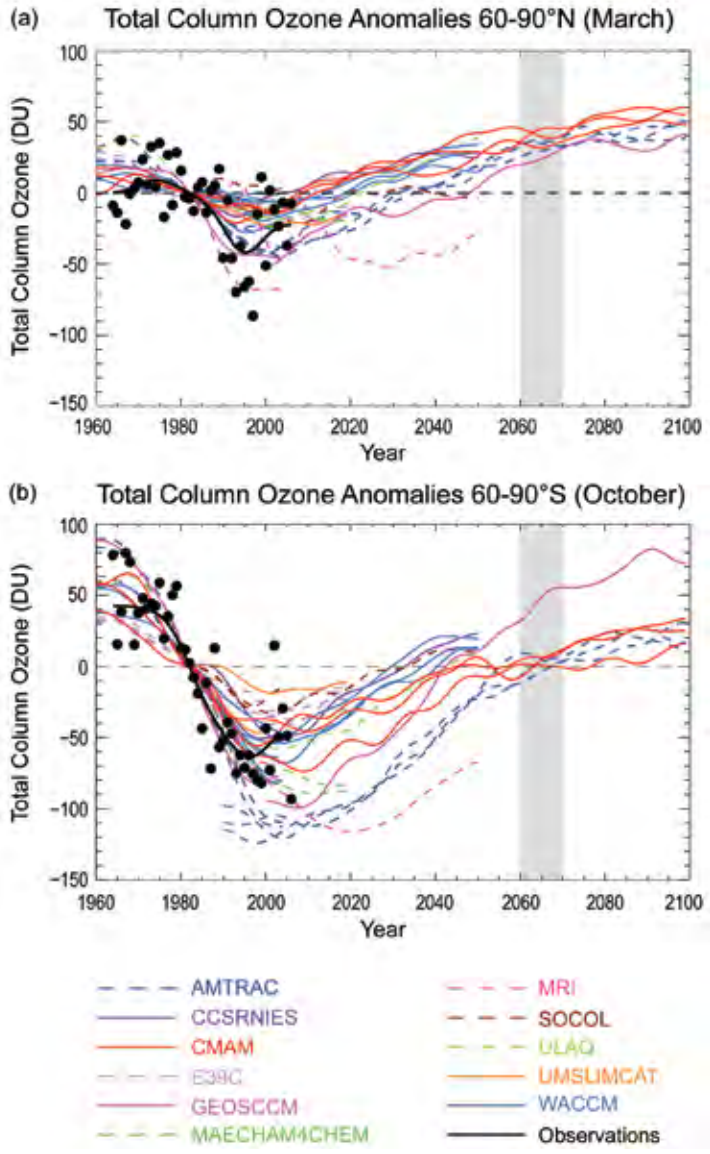

Figure 5.3 Zonal mean monthly ozone anomalies for the Arctic in March (panel a) and Antarctic in October (panel b). The figure is based on Figure 7 in Eyring *et al.* (2007), which was updated to include additional results after the publication of the WMO (2007) report. The observations are shown as black dots and a smooth curve representing the mean value. The grey vertical band marks the time period when polar EESC is expected to recover to the 1980 value.

In the context of the rest of this chapter (Sections 5.4 and 5.5), the most important attribution issue is whether EESC is a good proxy for future ozone behavior so that one could have confidence that policy decisions based on reducing EESC would achieve the goal of similar reductions in ozone depletion. Indeed, there are concerns (*e.g.*, Hadjinicolaou *et al.*, 2005) that improper interpretation of the recent

observed ozone increase after the late 1990s may give the wrong impression that the effects of halogens on ozone have been overestimated and one should relax the reduction strategy.

Chapter 6 in WMO (2007) identifies other factors that could complicate the attribution of the observed changes. These include changes in atmospheric composition of ozone-relevant compounds other than the halogens, changes in temperature and transport circulation, changes in solar cycle, and volcanic eruptions. The largest effect on the short-term (five to ten years) trend is expected to come from changes in transport circulation. The study of Yang *et al.* (2006) concluded that half of the observed increase in ozone between the late 1990s and 2005 could be attributed to changes in transport circulation in the lower stratosphere. This is not unexpected because, while EESC has stopped increasing, it essentially remained unchanged during this period. Hadjinicolaou *et al.* (2005) had a similar conclusion using a very different approach. The authors use a 3-D CTM to calculate the ozone from 1979 to 2003. The CTM uses the transport circulation from the ERA-40 analyses of the European Centre for Medium-range Weather Forecasting (ECMWF). The ozone chemistry is parameterized with the local loss frequency fixed at the 1980 conditions. The conclusion is that the ozone trends between 1994 and 2003 derived from the modeled and observed ozone agree, indicating that change in transport is the main driver in this time period. The paper also concluded that the model-calculated ozone (again with fixed loss frequency) showed a decreasing trend between 1979 and 1993, and the trend is around one-third of the trend derived from observation. More analyses (such as additional model results using full chemistry to show that the combined trend due to changes in transport and halogen loading is not significantly larger than the observed trend) are needed to support this last conclusion that changes in transport are responsible for one-third of the observed ozone trend between 1979 and 1993.

After 2050, effects from other changes (changes in CH_4, N_2O, and CO_2) will dominate. If the desire is to understand future ozone behavior beyond the effects of halogens, one must focus on the trends of the other ozone-relevant source gases and try to determine to what extent one could separate the effects on ozone in the future observations.

If all other factors remain constant, the future ultraviolet (UV) trend will depend on the anticipated ozone change.

5.3 EXPECTED RESPONSE IN SURFACE UV

Ozone column in the atmosphere is one of many factors that affect UV at the ground. The UV community emphasizes the importance of variations in aerosol, clouds, and surface albedo on UV. The effect of ozone change on clouds through climate feedback has not been quantified at this point, but is expected to be small.

If everything else is assumed to be constant, the future UV trend will depend on the anticipated ozone change. Within the limitation that applies to EESC as a proxy for future ozone behavior, it can likewise be used as a predictor for UV. However, most UV predictions are done locally at specific latitudes, thus the relationship between EESC and typical midlatitude ozone depletion is not particularly useful due to the other factors affecting UV. In practice, model-simulated ozone changes at specific latitudes are fed into a radiative transfer model to compute the change in UV irradiance. An example of such a calculation is shown in Figure 5.4, which shows the calculated noon-time erythemal irradiance at several latitudes. Note that the recovery at the southern polar latitude occurs much later than the midlatitude values, reflecting similar behavior of midlatitude and polar ozone columns as indicated in the results from the AMTRAC model in Figure 5.2.

5.4 FUTURE SCENARIOS FOR ODSs AND THEIR REPLACEMENTS

5.4.1 Baseline Scenario

In general, the historical portion of the baseline (A1) scenario is based on the observed mixing ratio time series, while future emissions are estimated using the most current information regarding expected future demand of ODSs, future banks (the amount of a chemical that has been produced but not yet emitted or chemically altered; see Box 2.5 in Chapter 2 for a more detailed definition), and current constraints placed by the Montreal Protocol.

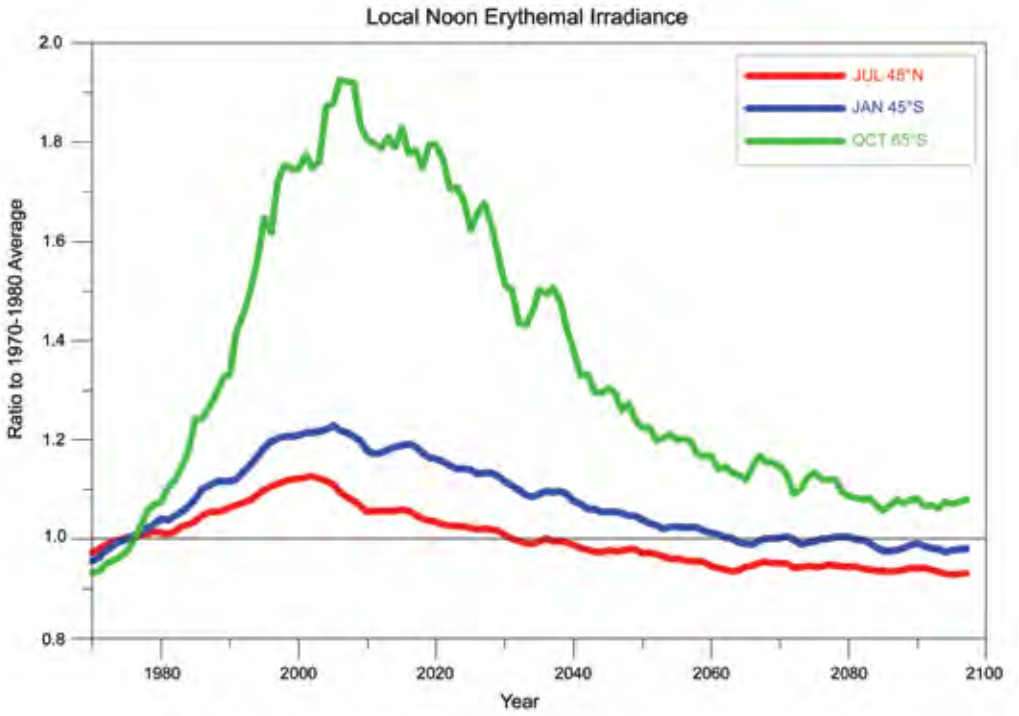

Figure 5.4 Estimated changes in erythemally weighted surface UV irradiance at local noon in response to projected changes in total column ozone as calculated by the AMTRAC CCM (see blue dashed curve in Figure 5.2) for the period 1970 to 2099, using zonal-averages in total ozone in the latitude bands 35°N-60°N, 35°S-60°S, and 60°S-90°S, and the solar zenith angle corresponding to 45°N in July, 45°S in January, and 65°S in October, respectively. At each latitude, the irradiance is expressed as the ratio to the 1970 to 1980 average. The results have been smoothed with a five-year running mean filter to remove some of the year-to-year variability in the ozone predictions in the model.

While this scenario consists of reasonable assumptions about the future, it does not represent a prediction, and future levels could be higher or lower depending on, for example, future policy actions and consumer choices. However, it represents a useful projection that is used to examine the sensitivity of ODS abundances to choices concerning future production, banks, and emissions.

The mixing ratios used to calculate the historical emissions are obtained primarily from atmospheric observations made by the NOAA Earth System Research Laboratory/ Global Monitoring Division (ESRL/GMD) (formerly Climate Monitoring and Diagnostics Laboratory, [CMDL]), the Advanced Global Atmospheric Gases Experiment (AGAGE), and the University of East Anglia (for halon-1211). South Pole firn observations are also considered for methyl chloride (CH_3Cl) and methyl bromide (CH_3Br) emissions before 1996. A box model is used to determine the emissions of the species for each year through 2005 using the observed mixing ratio time series and its current best estimate of the steady state global lifetime. Hence, when the same box model and lifetimes are used to calculate the surface mixing ratios from the derived emissions, they produce mixing ratios in the baseline scenario that are exactly equal to the observationally based time series given in Table 8-5 of WMO (2007). The same box model and lifetimes are used to derive the mixing ratio of each species after 2005 based on projected emissions.

Projections of future demand and sizes of banks are taken from IPCC/TEAP (2005), and play a major role in the calculation of future emissions. Details relating to the production and emission projections can be found in WMO (2007). The use of future demand and bank sizes from IPCC/TEAP (2005) in WMO (2007) represents an important departure from the approach used in previous WMO reports. Previously, the evolution of the estimated bank sizes was calculated solely using the difference between estimated annual production and emission. This approach had the potential to lead to accumulating large errors in the bank

Bank estimates of ozone-depleting substances are based on inventories of equipment containing these substances, an approach called the "bottom-up" method.

sizes because the bank often represents a small difference between the two relatively large production and emission values. The IPCC/TEAP (2005) bank estimates, however, are based on inventories of equipment, an approach often referred to as a "bottom-up" method. Hence, these estimates are independent of systematic errors in production or emission. It is believed that this new approach has led to better projections of future emissions.

Comparisons between future emissions projections of WMO (2003) and WMO (2007) demonstrate that the most substantial differences arise for CFC-11, CFC-12, carbon tetrachloride (CCl_4), and the HCFCs. The increase in the CFC emissions in WMO (2007) is primarily due to larger bank estimates of the bottom-up approach than were estimated by WMO (2003). The greatest HCFC emission difference is for HCFC-22 and is due to the substantially larger estimated future consumption of this compound by Article 5(1) countries. Current and projected future carbon tetrachloride emissions are now estimated to be higher than those projected in WMO (2003) based on observed mixing ratios consistent with a smaller decrease in emissions over the last few years and the continued inability to account for all CCl_4 emissions. The resulting differences in mixing ratios are discussed in Section 5.4.3.

5.4.2 Alternate Scenarios

Alternative scenarios and test cases were examined in WMO (2007) to quantify the relative effects of making various production and/or direct emissions reductions on EESC. Three cases for different ODS groups are designed to address three issues: (1) no future emission; (2) no future production; and (3) eliminations of the 2007 bank. Results from the "no future emission" case provide the future mixing ratios due to the decay of the ODSs already in the atmosphere only. This case represents the greatest theoretically possible reduction in the future atmospheric burden of the particular compound (short of processing the air to remove the ODSs). The "no future production" case quantifies the importance of new production relative to future emissions, while the "bank elimination" quantifies the benefit of the one-time sequestration and destruction of the 2007 global bank for future emissions. Additional cases are presented here that examine the effect of recovering and destroying the total estimated U.S. bank and the U.S. accessible bank in 2009. Estimates of these bank sizes and the technique used by the U.S. Environmental Protection Agency (EPA) to calculate these estimates are discussed in Chapter 2.

WMO (2007) also examined three alternative cases involving CH_3Br. Two cases involved removing quarantine and pre-shipment uses from 2015 onward and continuing Critical Use Exemptions at 2006 levels into the future. The third case explored the importance of the assumption that the 1992 anthropogenic emissions represented 30% of the total. Recent mixing ratio observations have suggested that this might be an overestimate with a more accurate percentage falling somewhere between 20% and 30%. These results are presented later in Section 5.5 and in Table 5.2.

A scenario based on the mitigation scenario described in IPCC/TEAP (2005) is also examined to quantify the effect of this carefully considered set of future policy options. The mitigation scenario only has a substantial effect on the bank of HCFC-22 in the scenario considered here.

After the WMO (2007) report and IPCC (2007) reports were written, the Parties to the Montreal Protocol voted to strengthen the HCFC regulations on both Article 5(1) and non-Article 5(1) countries. Approximations for the effect of this strengthening are discussed in Section 5.5.1.1.

5.4.3 Time Series of Source Gases

The mixing ratios of the current baseline scenario are compared with those of the WMO (2003) baseline scenario, and the "no future production" and "no future emission" test cases in Figure 5.5. The differences between the WMO (2007) and WMO (2003) baseline scenarios are apparent for several gases, with the differences for HCFC-22 particularly apparent. More modest, but also important are the differences for CFC-11 and CFC-12. The HCFC-22 difference is due to the increase in the expected future consumption of Article 5(1) countries of the Montreal Protocol, while the

increase in the CFCs is due to the larger bank size estimates of IPCC/TEAP (2005). HCFC-141b, HCFC-142b, and halon-1301 show reduced mixing ratios in the short term compared to WMO (2003) owing to the reduced observed growth rates between 2001 and 2004 and the expectation of lower future emissions.

The importance of future projected production and bank sizes to future emissions is also apparent for the various compounds. For example, the "no future production" curve for CFC-12 is only slightly different from the baseline curve; hence the bank of CFC-12 is expected to dominate future emissions, with its effect represented by the difference between the "no future emission" and "no future production" curves. The relative importance of future production compared to the amount in the banks varies strongly among the ODSs, with the future abundances of CFC-11 depending primarily on its bank size and HCFC-22 future abundances depending primarily on future production. No bank is considered in the future projections of methyl chloroform (CH_3CCl_3), CCl_4, and CH_3Br.

5.5 CHANGES IN INTEGRATED EESC AND RADIATIVE FORCING

5.5.1 Time Series of EESC

5.5.1.1 Midlatitudes

The evolution of ODS mixing ratios cannot, by themselves, be used to accurately quantify the ozone destruction due to those ODSs. The established relationship between stratospheric ozone depletion and inorganic chlorine and bromine abundances suggest that the temporal evolution of inorganic chlorine- and bromine-species in the stratosphere is an important indicator of the potential damage of human activity on the health of stratospheric ozone. Equivalent Effective Stratospheric Chlorine (EESC) was developed to relate this halogen evolution to tropospheric source gases in a simple manner (Daniel *et al.*, 1995; see also Box 2.7 in Chapter 2). This quantity sums ODSs, accounting for a transit time to the stratosphere, for the number of halogen atoms in the ODS, for the greater per-atom potency of stratospheric bromine (Br) compared to chlorine (Cl) in its ozone destructiveness with a constant factor (α), and also includes the varying rates with which

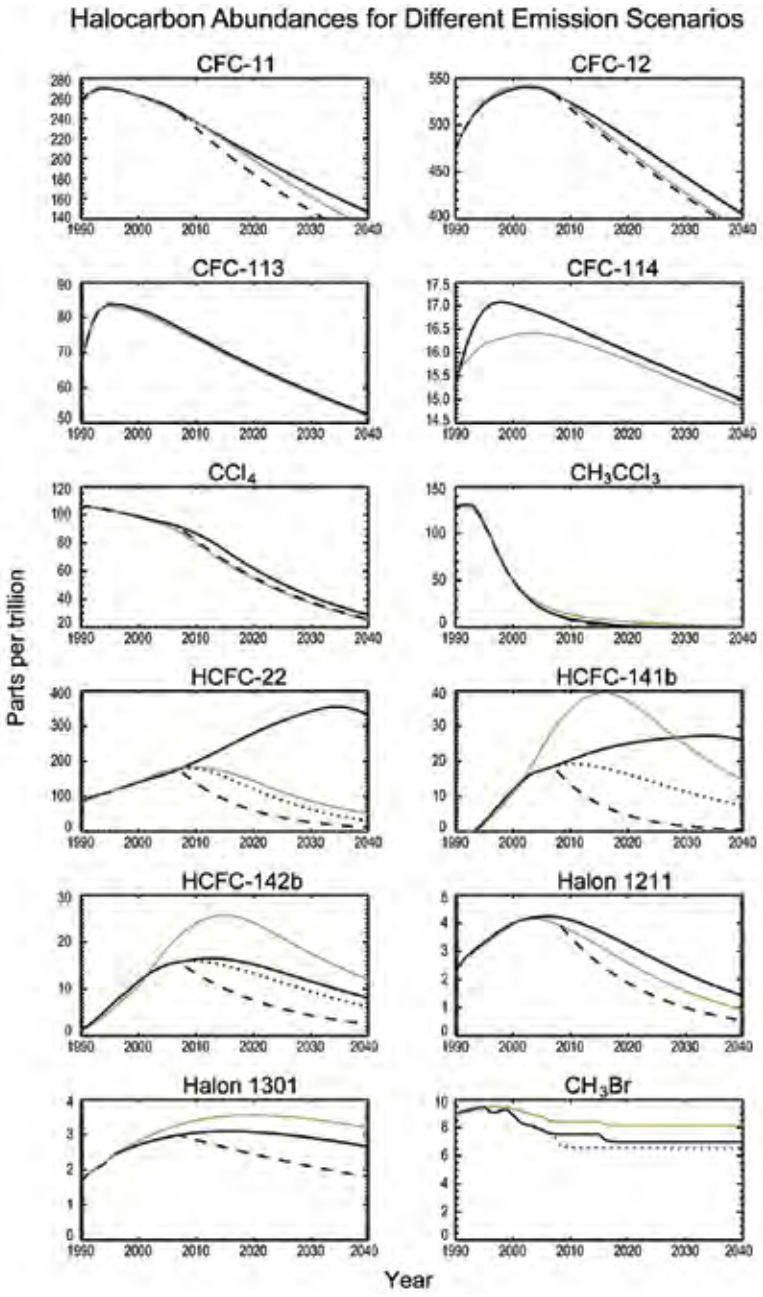

Figure 5.5 Mixing ratio comparisons of the WMO (2007) baseline scenario (solid black) with the baseline scenario from WMO (2003) (green), the "no future emission" test case (dashed), and the "no future production" case (dotted curve). The figure is based on Figure 8-2 in WMO (2007). Note that different vertical scales are adopted for sub panels and some of the plotted values do not start from zero. For several of the gases, the solid black curve obscures the dotted or dashed curves.

Cl and Br will be released in the stratosphere from different source gases. EESC has been used as a proxy for the effect of human-produced ODS abundances on future ozone depletion (WMO, 1995, 1999, 2003, 2007). The values for midlatitude EESC discussed here were calculated for WMO (2007) from the global averaged surface mixing ratios for the ODSs, using a constant lag time of three years

and release factors given in the same report. Recent development on how to apply EESC to polar ozone and refinements in using the mean age of air will be discussed in Sections 5.5.1.2 and 5.5.2, respectively.

The relative contribution of various ODSs and ODS groups to midlatitude EESC are shown as a function of time from 2000 to 2100 on the left-hand side of Figure 5.6. The prominent role of CFCs today and into the future is apparent. The slow decline of the contribution from CFCs is primarily due to the relatively long atmospheric lifetimes of the species in this group of compounds and what is already in the atmosphere, and not to continued emission, although continued emission does play a small role. The importance of the halons and CH_3Br, all bromine-containing source gases, is also clear even though their atmospheric concentrations are substantially smaller than those of the chlorine-containing ODSs. This is because stratospheric bromine is much more effective per atom than chlorine for stratospheric ozone destruction. As stated in Chapter 2, WMO (2007) has estimated that an atom of bromine is 60 times more effective than an atom of chlorine for global stratospheric ozone destruction. The lower panels show the change in EESC due to the elimination of production and emission for CFCs, HCFCs, halons, and CH_3Br.

In late 2007, the Montreal Protocol HCFC restrictions for both production and consumption were strengthened, partly in response to the renewed awareness of the importance of HCFCs to climate forcing in addition to ozone depletion.

In the past, EESC estimates have been used to evaluate various ODS emissions scenarios primarily using two metrics. They are: (1) a comparison of the times when EESC returns to 1980 levels, the EESC RD; and (2) the relative integrated changes in EESC between 1980 or the current time and the corresponding EESC RD. Figure 5.7 demonstrates that the return of midlatitude EESC to the 1980 level is currently expected to occur around 2049 for the baseline scenario, five years later than projected in WMO (2003). This later return was primarily ascribed to higher estimated future emissions of CFC-11, CFC-12, and HCFC-22. The increase in CFC emissions is due to larger estimated current bank sizes, while the increase in HCFC-22 emissions is due to larger estimated future production. The soonest that a complete theoretical elimination of emissions could lead to a return to 1980 levels is 2034. Elimination of all future ODS production is expected to lead to a return to 1980 EESC levels in 2043, while an elimination of the 2007 bank is expected to lead to a return in 2041.

A detailed partitioning of the effects of reductions in the various ODS groups is shown in Table 5.2. The years when EESC is expected to return to 1980 levels are also included in the table for midlatitudes and for the Antarctic vortex. The Antarctic ozone response to EESC will be discussed in more detail in Section 5.5.1.2. The table illustrates that the elimination of the future emissions of CFCs, HCFCs, and halons represents the greatest potential for reducing future ozone depletion. To accomplish this elimination for CFCs and halons, banks would have to be captured and destroyed because future emission is expected to be dominated by the release from banks. For HCFCs, future production plays a larger role in future emission than do the current banks, so emissions from both banks and future production would have to be eliminated. The technical difficulty and expense involved with capturing banks depends on the nature of the banks, while the feasibility of reducing future production will depend on replacement options for the pertinent applications. More details concerning the nature of the various ODS uses and bank types and the options available for reducing future ODS emissions can be found in other reports, including IPCC/TEAP (2005) and UNEP/TEAP (2007). It should also be recognized that these full bank recovery and zero production and emission test cases shown in Table 5.2 are meant as hypothetical cases against which more realistic scenarios can be compared. This procedure is used in Section 5.6 to evaluate the significance of the United States ODS banks.

The results for the scenario representing the IPCC/TEAP (2005) mitigation scenario are not shown in Table 5.2, but this scenario leads to an EESC response that is approximately 20% of the zero-emission case for the HCFCs, due primarily to actions that would reduce the HCFC-22 bank emission.

Future emissions of CH_3Br also have the potential to be as important as each of these three classes of compounds. The continuation

Table 5.2 Comparison of scenarios and cases[a]: the year when EESC drops below the 1980 value (*i.e.*, EESC RD) for both midlatitude and polar vortex cases, and integrated EESC differences (midlatitude case) relative to the baseline (A1) scenario.

Scenario	Percent Difference in integrated EESC relative to baseline scenario for the midlatitude case		Year (x) when EESC is expected to drop below 1980 value	
	Midlatitude			Antarctic Vortex[b]
	$\int_{1980}^{x} EESC\,dt$	$\int_{2007}^{x} EESC\,dt$		
Scenarios				
A1: Baseline Scenario			2049	2065
Cases[a] of zero production from 2007 onwards of:				
All ODSs	−8.0	−17.1	2043	2060
CFCs only	−0.1	−0.3	2049	2065
Halons only	−0.2	−0.5	2049	2065
HCFCs only	−5.5	−11.8	2044	2062
Anthropogenic CH_3Br only	−2.4	−5.1	2048	2063
Cases[a] of zero emissions from 2007 onwards of:				
All ODSs	−19.4	−41.7	2034	2050
CFCs only	−5.3	−11.5	2045	2060
CH_3CCl_3 only	−0.1	−0.2	2049	2065
Halons only	−6.7	−14.4	2046	2062
HCFCs only	−7.3	−15.7	2044	2062
CCl_4 only	−1.3	−2.9	2049	2065
Anthropogenic CH_3Br only	−2.4	−5.1	2048	2064
Cases[a] of full recovery of the 2007 banks of:				
All ODS	−12.9	−27.8	2041	2057
CFCs only	−5.2	−11.3	2045	2060
Halons only	−6.7	−14.3	2046	2062
HCFCs only	−1.9	−4.1	2048	2065
CH_3Br sensitivity:				
Same as A1, but CH_3Br anthropogenic emissions set to 20% in 1992[c]	3.1	6.6	2051	2068
Same as A1, but zero QPS production from 2015 onwards	−1.5	−3.2	2048	2064
Same as A1, but Critical Use Exemptions continued at 2006 level	1.9-2.2	4.0-4.7	2050	2067

[a] Importance of ozone-depleting substances for future EESC were calculated in the hypothetical "cases" by setting production or emission of all or individual ODS groups to zero in 2007 and subsequent years or the bank of all ODS or individual ODS groups to zero in the year 2007 alone. These cases are not mutually exclusive and separate effects of elimination of production, emissions and banks are not additive.

[b] Calculated using a lag time of six years and the same release factors as in midlatitudes.

[c] In the baseline scenario this fraction was assumed to be 30% in 1992 with a corresponding emission fraction of 0.88 of production. In this alternative scenario an anthropogenic fraction was assumed to be 20% with an emission fraction of 0.56 of production. In both scenarios the total historic emission was derived from atmospheric observations and a lifetime of 0.7 years.

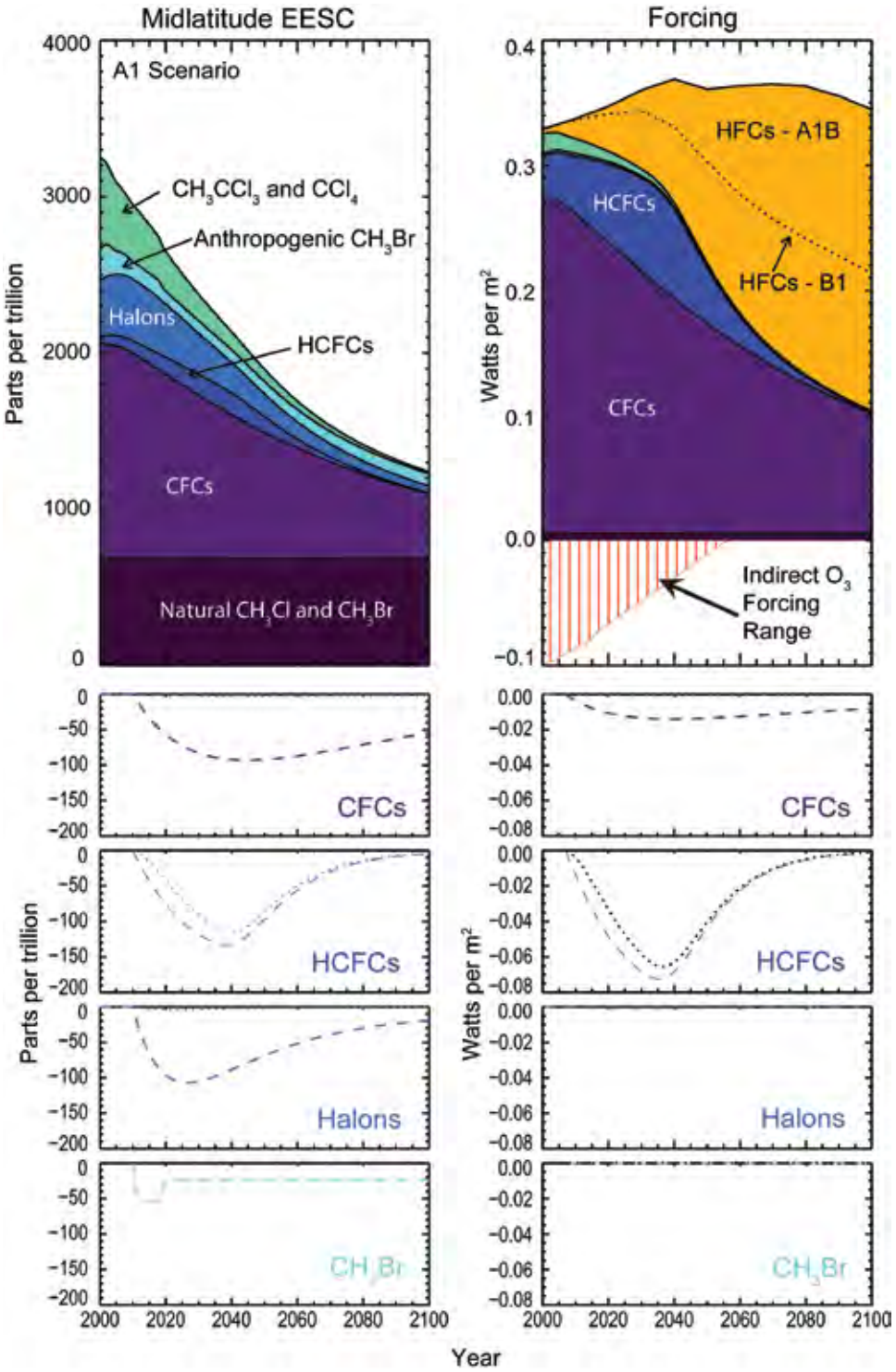

Figure 5.6 EESC and direct radiative forcing estimates from 2000 to 2100 for the A1 baseline scenario in WMO (2007) (upper panels), and expected decreases relative to the baseline scenario due to a cessation of emission (dashed curves) and production (dotted curves) in 2007 for CFCs, HCFCs, halons, and anthropogenic CH_3Br. The figure is adapted from Figure 8-5 in WMO (2007) except for the addition of the indirect forcing in the upper right hand panel. Note the difference in the vertical scales between the top panel and the bottom four panels. The "no production" curve for CFCs and halons lies almost on the zero line, indicating that future productions of these ODSs play a very small role in the baseline scenario. In contrast, the contribution from the HCFCs is mostly due to future productions. The "no emission" and "no production" curves are identical for CH_3Br because no bank was considered in its projections. The HFC forcing is shown for the B1 and A1B SRES scenarios. The indirect forcing due to ozone depletion caused by ODSs is included for comparison, but should be considered only a rough approximation owing to reasons discussed in the text of this chapter and of Chapter 2.

of the Critical Use Exemption at the 2006 level and the continuation of QPS uses both have a substantial impact on global EESC.

In late 2007, the Montreal Protocol HCFC restrictions for both production and consumption were strengthened, partly in response to the renewed awareness of the importance of HCFCs to climate forcing in addition to ozone depletion. While restrictions were tightened for both Article 5(1) and non-Article 5(1) countries, the changes for the Article 5(1) countries are much more significant for stratospheric ozone. In Figure 5.8, the former Protocol HCFC restrictions for Article 5(1) countries are compared to the newly adopted ones, as well as to the United States proposal that contributed to the strengthened restrictions. An additional curve is also shown that represents the closest scenario calculated in UNEP/TEAP (2007). For the TEAP scenario, it is estimated that integrated EESC is reduced by 2.6% and 5.6%, respectively, for the integration from 1980 to the return of EESC to 1980 levels and from 2007 to the return to 1980 levels. This is a substantial reduction even when compared to the zero emissions case for HCFCs in Table 5.2. The baseline HCFC emissions are slightly higher in UNEP/TEAP (2007) than those assumed in WMO (2007), making the effect of HCFC reductions correspondingly slightly higher. This TEAP report also examines other "practical options" that could be usefully employed to reduce future emissions of HCFCs and other ODSs. These include emission reduction measures during the use phase of applications and equipment, design and material section alternatives, end-of-life management, and early retirement of equipment. These measures were submitted by the Parties to the Montreal Protocol and organized at the 26th Open-ended Working Group Meeting of the Parties to the Montreal Protocol. The TEAP report finds that a combination of earlier HCFC phase-out described above with these additional "practical measures" leads to an integrated EESC reduction of 7.4% and 16.0% percent, respectively, for the integration from 1980 to the return of EESC to 1980 levels and from 2007 to the return to 1980 levels.

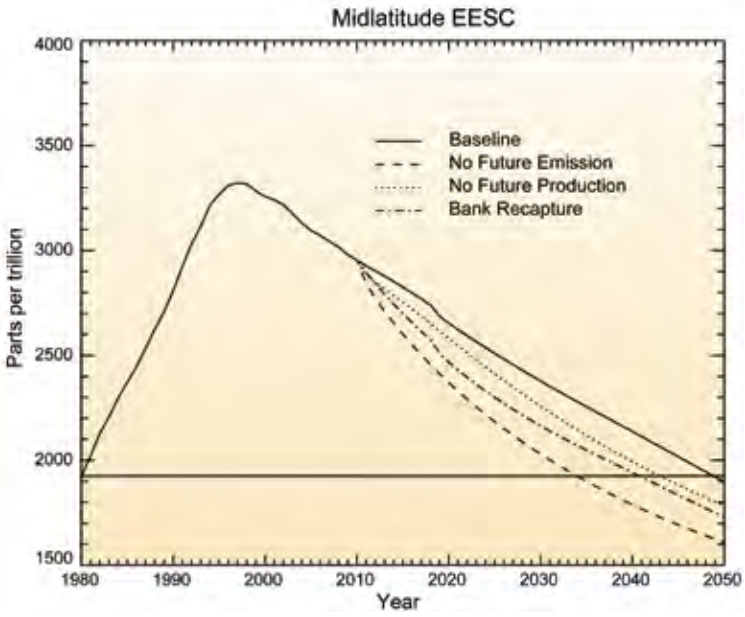

Figure 5.7 Midlatitude EESC estimates from 1980 through 2050 for the baseline scenario and the three comparative test cases considered in WMO (2007). The horizontal line represents the 1980 EESC level. This figure is redrawn from Figure 8-4 of WMO (2007).

For midlatitudes, the test case involving elimination of all future ozone-depleting substance production is expected to lead to 1980 Equivalent Effective Stratospheric Chlorine levels in 2043.

5.5.1.2 Polar Regions

Compared to midlatitude EESC, Arctic EESC is less useful as a proxy for polar ozone depletion because interannual variability in meteorology has a much larger impact on the ozone response

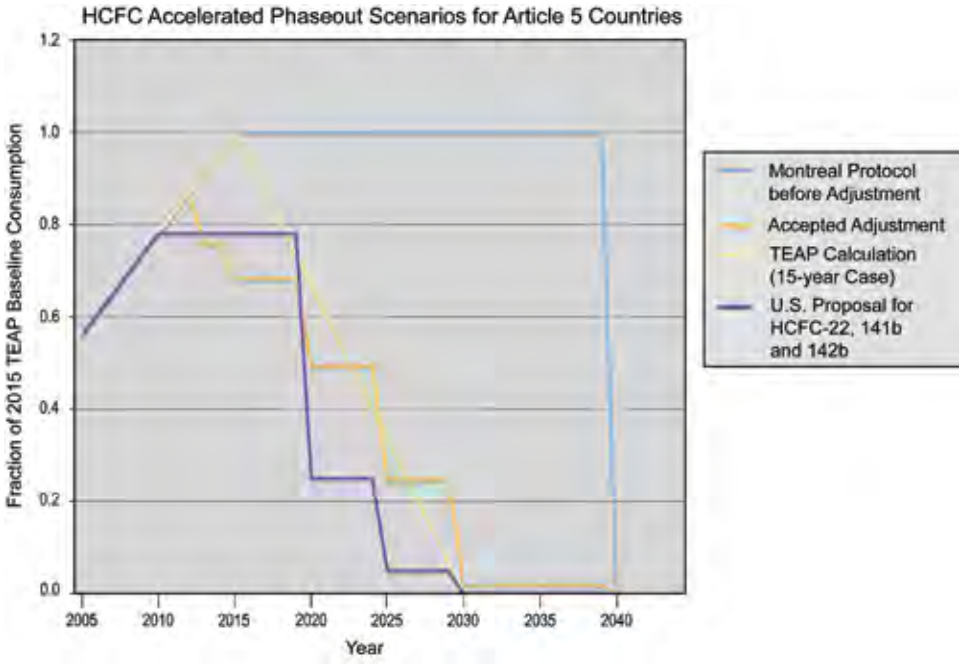

Figure 5.8 Comparison of alternate scenarios for future emissions of HCFCs.

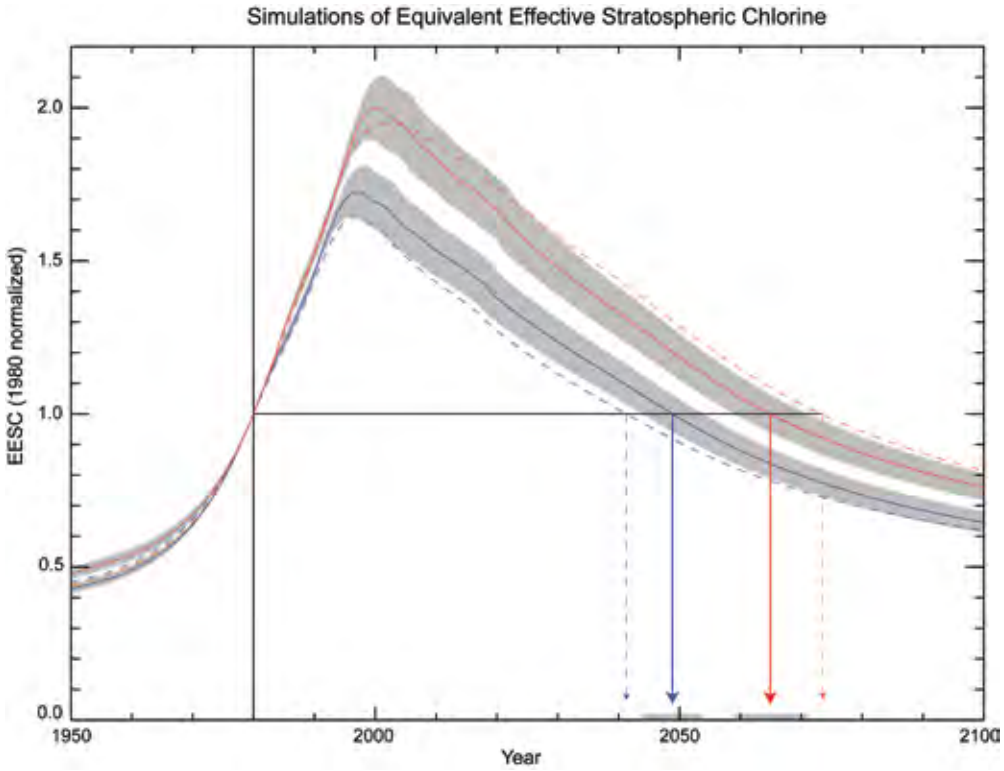

Figure 5.9 Comparison of EESC values calculated using a lag time and fixed fractional release values (solid) vs. those calculated using a mean age with an age spectrum and fractional release values parameterized as functions of mean age (dashed). The blue curves are for midlatitudes and are calculated with a mean age and lag time of three years. The curves for the polar region are in red and are calculated with a mean age and lag time of six years.

to inorganic halogen loading. In the core of the Antarctic vortex during early spring, the interannual variability is smaller, suggesting that EESC could provide a useful proxy for ozone hole recovery (Newman *et al.*, 2006). The far right column in Table 5.2 shows the results calculated using a time lag of six years and the same release factors based on midlatitude measurements. Because of the larger time-lag, the polar EESC value in 1980 is smaller than the 1980 midlatitude value. In addition, the larger lag time also makes the polar EESC value larger than the midlatitude EESC value in 2050. Therefore, the polar EESC RD is 15 to 17 years later than the midlatitude EESC RD.

5.5.2 EESC and Mean Age of Air

Previous EESC calculations have not included a distribution of transport times from the tropopause into the stratosphere (the so called age-of-air spectrum) or any dependence of the fractional chlorine release value on the age-of-air. Newman *et al.* (2006) reformulated EESC to account for both an age-of-air spectrum and age-dependent fractional release rates. Those results were discussed in Box 8-1 of WMO (2007). In this section, we will summarize how the EESC estimates derived from Newman *et al.* (2006) differ from the results in Section 5.5.1.2.

The dashed lines of Figure 5.9 show EESC for mean ages of three years (blue) and six years (red) as estimated using the Newman *et al.* (2006) technique, while the solid lines show EESC for constant age shifts (time-lags) of three years (blue) and six years (red). The solid lines duplicate the EESC used in WMO (2007). The main difference in the recovery dates between the two methods in each case (midlatitude and polar) is a result of the differences in fractional release values. In the WMO (2007) case, the release factors are fixed values, while the release factors in the Newman *et al.* (2006) curves are mean-age dependent. Note that the Newman *et al.* (2006) release factors at midlatitudes lead to smaller EESC values relative to 1980 levels than the values used in WMO (2007) and that an earlier EESC RD is projected. In contrast, the Newman *et al.* (2006) release factors at the

pole for the six-year mean age are larger than the WMO (2007) values, and result in a later EESC RD.

Newman *et al.* (2006) raised the issue of the uncertainty in predicting the EESC RD associated with the choice of mean age and release factors to represent midlatitude and polar conditions. While the use of different mean ages would change the absolute timing of the recovery for the baseline case and other test cases, we are reasonably confident that it would not change the conclusion about the relative effects of different test cases.

5.5.3 Time Series of Radiative Forcing

To adhere to the requirements of the Montreal Protocol, several courses of action have been adopted, including not-in-kind replacements of ODSs and changes in operations that reduce emissions. Applications that previously used CFCs are now performed with CFC replacements, HCFCs and HFCs, with HFCs likely to play a larger role in the future as HCFCs are phased out by the Montreal Protocol. Because HFCs contain no chlorine, bromine, or iodine, they do not destroy stratospheric ozone and therefore are not considered in WMO (2007). Furthermore, because future HFC emissions and production are not regulated by the Montreal Protocol, as are HCFCs, future projections of HFC concentrations are generally much more uncertain than those of ODSs and are heavily dependent on future economic growth assumptions and policy decisions. The forcing from HFCs will be included here as part of the discussion. However, it should be pointed out that the replacement strategy may also involve changes in other greenhouse gas emissions associated with the life cycle analyses (IPCC/TEAP, 2005). The change in forcing associated with those greenhouse gases is not included in the discussion.

Once the mixing ratio time series has been determined, it is a simple matter to estimate the future direct radiative forcing due to the various compound groups from the radiative efficiencies of each ODS (WMO, 2007). This forcing time series, calculated by multiplying the mixing ratio time series by the radiative forcing efficiencies of the particular ODSs, is shown on the right-hand side of Figure 5.6. Direct radiative forcing from ODSs and HFC replacement chemicals is approximately 0.34 W per m^2 in 2005 and is expected to stay below 0.4 W per m^2 through 2100 (according to the WMO (2007) scenario for ODSs and SRES A1B and B1 scenarios for HFCs). This is to be compared with forcing from CO_2 of 1.66 W per m^2 in the 2005 atmosphere, increasing to as high as 5 W per m^2 by 2100 for the SRES A1B scenario. The continued importance of the CFCs, along with the importance of the HCFCs, are perhaps the most striking features of this figure. The direct forcing contributions of the halons and CH_3Br are small because of their small atmospheric mixing ratios. The effect of the bromocarbons on ozone depletion is enhanced because of the higher per-atom efficiency of bromine compared to chlorine in destroying ozone; such a chemically-caused enhancement does not apply to radiative forcing.

The potential reduction in direct forcing due to the elimination of future production and emission is shown for CFCs, HCFCs, halons, and CH_3Br in the lower four panels of Figure 5.6. Overall, direct forcing from CFCs is expected to decrease to 0.1 W per m^2 by 2100. Direct forcing from HCFCs and other ODSs are expected to be negligible by 2100. It is evident that elimination of future HCFC emission has the largest effect on radiative forcing of the ODSs among the test cases considered here. This peak forcing reduction of almost 0.07 W per m^2 in 2040 represents slightly less than 5% of the CO_2 radiative forcing in 2000 and less than half of the N_2O radiative forcing in 2000. In comparison, elimination of future CFC emissions will bring about a reduction of 0.015 W per m^2 in 2040.

The forcing of the HFCs, generally used as replacements for the ODSs, are included in the figure as the orange shaded region for the SRES (Nakićenović *et al.*, 2000) A1B scenario. The line within the orange region represents the alternate forcing of the HFCs in the B1 SRES scenario. Atmospheric observations suggest that the 2000 forcing due to the HFCs is slightly larger than that estimated by the SRES scenarios, primarily due to the higher abundances of HFC-23 observed. Projected forcing from HFCs is 0.15 W per m^2 and 0.24 W per m^2 in 2050 and 2100, respectively, for

To adhere to the requirements of the Montreal Protocol, several courses of action have been adopted, including not-in-kind replacements of ozone-depleting substances and changes in operations that reduce emissions.

the SRES A1B scenario, while other scenarios indicate that it will be lower.

The direct forcing of the ODSs provides only a partial story of their total radiative forcing. Their destruction of ozone leads to an additional, indirect forcing that is thought to be significant but remains highly uncertain. An estimate of the indirect forcing from the ODSs is shown in Figure 5.6 as the red hatched region. It represents an uncertainty range of ±100% around the best estimate for the period 1979-1998 (*i.e.*, −0.05±0.05 W per m^2), taken from IPCC (2007). While the ozone forcing itself is highly uncertain, additional uncertainties exist that are not quantified here associated with, for example, the simplifying assumption of a linear relationship between ozone depletion and EESC above the 1980 threshold and even the amount of the observed ozone trend that is due to ODSs. The central forcing value (−0.05 W per m^2) suggests that ozone depletion offsets about one-sixth of the total direct ODS forcing around 2000. This figure also shows that the indirect forcing will gradually diminish in the coming decades, and is expected to return to near zero around 2050 as ozone becomes insensitive to the level of ODSs. This results from the assumption that the EESC value in 1980 represents a threshold, below which ozone depletion does not respond to changing EESC levels. While such a picture is likely imperfect, global ozone data do suggest that the response of ozone to EESC may have changed at this EESC level. Finally, there have been studies suggesting that ozone radiative forcing may lead to a substantially different temperature response than does the same radiative forcing change from CO_2 (Joshi *et al.*, 2003 and references therein). Such a situation would imply that direct and indirect radiative forcing comparisons, as shown in Figure 5.6, could be misleading in estimating climate response. Additional details concerning the indirect forcing of the ODSs due to ozone depletion can be found in Chapter 2, particularly in Box 2.2. Accurate quantification of this forcing and of indirect GWPs currently represents a scientific gap due to the significance of the associated uncertainties.

In addition to direct forcing by ozone-depleting substances, the destruction of ozone by ozone-depleting substances also leads to an indirect forcing that is thought to be significant but remains highly uncertain.

5.6 UNITED STATES CONTRIBUTIONS TO EESC AND TO RADIATIVE FORCING BY ODSs AND THEIR REPLACEMENTS

Because of the long-lived nature of the ODSs, EESC and the radiative forcing arising from emissions of these compounds should be thought of as global quantities. This allows the contribution to midlatitude EESC and global radiative forcing to be apportioned to individual countries if their emissions are accurately known. As discussed in Chapter 2 in this Report, ODS production and consumption amounts for the United States are reported to the United Nations Environment Programme (UNEP), as required by the Montreal Protocol (UNEP, 2007). Data are also compiled by the Alternative Fluorocarbons Environmental Acceptability Study (AFEAS, 2007) for certain ODSs and for HFC-134a, although the amount reported to AFEAS has represented a smaller fraction of global production in the last decade or so when compared with the UNEP data. A discussion of the comparison of the data from these two compilations with observed atmospheric mixing ratio observations is provided in Chapter 2. Also in response to a requirement associated with the United States being a signatory to the Montreal Protocol, the U.S. EPA uses a vintaging model to estimate annual emissions from the estimated production and consumption values after 1985. Chapter 2 discusses the results from the U.S. EPA's vintaging model through the past and the assumptions made to estimate United States emissions prior to 1984. Here, we use these assumptions along with the U.S. EPA's projections to estimate future levels of source gases attributable to the United States and their contributions to both EESC and radiative forcing.

5.6.1 Contribution to EESC

It is useful to note that the EESC in 2030 will be 2400 ppt, with about one-third from the natural CH_3Cl and CH_3Br. For the remaining two-thirds attributed to manmade emissions, about 15% is due to emissions prior to 1975, and about 20% is due to emissions between 1975 and 1984. The contributions from United

Table 5.3 Comparison of global and United States bank elimination projections in terms of integrated EESC and EESC RD. The global test cases are taken from WMO (2007) and consider elimination of the global bank in 2007. U.S. cases assume elimination of the full U.S. bank, or the accessible U.S. bank in 2009.

Scenario	Percent Difference in integrated EESC relative to baseline scenario for the midlatitude case		Year (x) when EESC is expected to drop below 1980 value	
	Midlatitude			Antarctic Vortex
	$\int_{1980}^{x} EESC\,dt$	$\int_{2007}^{x} EESC\,dt$		
Scenarios				
A1: Baseline Scenario			2048.9	2065
Cases of full recovery of the 2007 banks[b] of:				
B0: All ODS (global)	−12.9	−27.8	2040.8	2056.7
CFCs (global)	−5.2	−11.3	2045.1	2060.4
CFC-11 (U.S., accessible)	−0.0[a]	−0.0[a]	2048.1	2064.1
CFC-12 (U.S., accessible)	−0.0[a]	−0.1	2048.9	2065.0
CFC-11 (U.S., total)	−1.1	−2.3	2048.1	2064.1
CFC-12 (U.S., total)	−0.3	−0.7	2048.7	2064.8
Halons (global)	−6.7	−14.3	2045.7	2062.0
halon-1211 (U.S., accessible)	−0.1	−0.2	2048.9	2065.0
halon-1301 (U.S., accessible)	−0.3	−0.6	2048.7	2064.8
halon-1211 (U.S., total)	−0.1	−0.2	2048.9	2065.0
halon-1301 (U.S., total)	−0.3	−0.6	2048.7	2064.8
HCFCs (global)	−1.9	−4.1	2048.4	2064.8
HCFC-22 (U.S., accessible)	−0.3	−0.6	2048.8	2065.0
HCFC-22 (U.S., total)	−0.3	−0.7	2048.8	2065.0
HCFC-141b (U.S., total)[c]	−0.4	−0.8	2048.8	2065.0
HCFC-142b (U.S., total)[c]	−0.1	−0.1	2048.9	2065.0

[a] Values reported as −0.0 are smaller than 0.05% in magnitude.
[b] Note that the U.S. numbers are for 2009 banks.
[c] Accessible bank values for HCFC-141b and HCFC-142b are not provided because the U.S. EPA estimates a zero accessible bank size for these compounds.

States emissions to the loading in 2030 due to manmade emissions are 4.5 to 9% from United States pre-1975 emissions, 2 to 9% from United States emissions between 1975 and 1984, and 9 to 19% from United States emissions after 1985. Summing the contributions, we estimate that in 2030 the midlatitude anthropogenic EESC amount resulting from United States emissions represents about 15 to 37% of the EESC amount resulting from all global anthropogenic emissions.

5.6.2 Contribution to Radiative Forcing by ODSs and Their Replacements

The United States' contribution to global direct radiative forcing from ODSs, HFCs, and PFCs is expected to be 19 to 41% by 2030. The lower end of this range remains roughly constant until 2030, while the upper end gradually declines from about 47% in 2010. As was done for the previous EESC contribution results, these forcing estimates are calculated only considering anthropogenic emissions. Future United States perfluorocarbon (PFC) and sulfur hexafluoride (SF_6) emissions, which are projected to contribute very little to future

The United States' contribution to global direct radiative forcing from ODSs, HFCs, and PFCs is expected to be 19 to 41% by the year 2030.

radiative forcing (less than 10^{-5} W per m^2 through 2030), are estimated from the U.S. EPA vintaging model, while the future global abundances of these compounds are taken from the A1B and B1 SRES scenarios (Nakićenović *et al.*, 2000). If global PFCs and SF6 were not considered in the radiative forcing calculation, United States emissions are projected to contribute about 20 to 43% of global radiative forcing by ODSs and their replacements in 2030.

5.6.3 Options for United States ODS Banks

The accessible and total bank size estimates for United States equipment and applications in 2005 are compared to global bank estimates from WMO (2007) in Table 5.3. Additional reduction cases are shown in Table 5.3 that quantify the importance of the recovery and destruction of United States total banks and United States accessible banks. The U.S. EPA has defined "accessible" banks as the quantity of ODSs that is contained in equipment (*i.e.*, fire protection equipment and refrigeration/air conditioning systems). Furthermore, it is assumed that the amount of ODS recoverable from this equipment is equal to the full equipment charge minus the average annual loss rate from leakage and servicing. It is possible that some of the non-accessible banks could be recovered and destroyed with appropriate policy measures, market-based incentives, and/or certain technological advances. Table 5.3 shows that the halon-1301 and HCFC-22 United States accessible banks are the most substantial in terms of contributing to potential future integrated EESC reductions. If the total United States banks are considered, CFC-11, HCFC-141b, CFC-12, HCFC-22, and halon-1301 banks are most important. The calculations for the United States halon banks do not include stockpiles, and so should be considered underestimates of the full potential benefit of recovering and destroying these banks.